Theory of hyperfine- and exchange-field distributions in amorphous speromagnets with application to amorphous yttrium iron garnet

M. E. Lines and M. Eibschütz
AT&T Bell Laboratories, Murray Hill, New Jersey 07974
(Received 19 April 1984)

The hyperfine-field distribution in amorphous speromagnetic $Y_3Fe_5O_{12}$ (yttrium iron garnet, YIG) is shown to result dominantly from local spin disorder via its supertransferred component H_{ST}. Since this same spin disorder determines local exchange fields H_{ex}, the hyperfine-field distribution indirectly contains much information concerning the distribution of H_{ex} in the "spin-glass" environment. A theory is presented which relates H_{ST} and H_{ex} through local spin disorder and in terms of which both the distributions of hyperfine and exchange fields can be represented in terms of a few common parameters. The theory, which should be directly applicable to a whole range of ferric amorphous insulators, is applied here to amorphous YIG and provides an excellent interpretation of the details of the observed hyperfine spectrum. From this fit we derive, via the theory, the predicted distribution of exchange fields in amorphous YIG. We find, in particular, that the mean exchange field $\langle H_{ex}\rangle$ is only some 6% of its equivalent in crystalline YIG in accord with the ~15-fold difference in spin-ordering temperatures between the crystalline amorphous phases.

I. INTRODUCTION

In spite of a wealth of experimental information now available concerning hyperfine-field distributions in amorphous magnetic materials, little progress has been made in the way of theoretical understanding. This is primarily because the hyperfine field H_{hf}, even in a well-defined crystalline environment, is in general the sum of several physically distinct contributions of comparable magnitudes each intimately related to separate aspects of the electronic structure.[1] In light of this complexity it seems appropriate to make initial efforts in the amorphous context for systems in which not all of these contributions are of comparable importance.

In this respect the amorphous ferric oxide and fluoride-based speromagnetic insulators are good candidates since experimental hyperfine distributions $p(H_{hf})$ of excellent quality are now becoming available and, for these, contributions to H_{hf} from orbital angular momentum and conduction-electron polarization are rigorously absent, while those from dipolar sources (H_{dip}) are small. This leaves only the "contact" field, proportional to the polarization of s-electron density at the nucleus in question, as relevant for these systems.

The contact field is the vector sum of a local part $\vec{H}_{loc}$ and a supertransferred part $\vec{H}_{ST}$. The former is proportional to the local $3d$ spin $\vec{S}_0$ on the ion under consideration (with spin quantum number $S=\frac{5}{2}$ for the case of ferric ions) while the latter is the resultant of contributions from all single-ligand-bridged ferric nearest neighbors n, each proportional to the electronic spin $\vec{S}_n$ on the neighbor site,[2,3] i.e.,

$$\vec{H}_{hf}=\vec{H}_{loc}+\vec{H}_{ST}+\vec{H}_{dip}\ , \tag{1.1}$$

$$\vec{H}_{loc}=-C(\vec{S}_0/S),\quad \vec{H}_{ST}=\sum_n B_n(\vec{S}_n/S)\ , \tag{1.2}$$

in which C and B_n are positive scalar field parameters and $|\vec{H}_{dip}| \ll |\vec{H}_{hf}|$. Of particular significance is the fact that an association with the geometry of coordination can be made through the known form which B_n takes as a function of the iron-ligand-iron bond angle ϕ_n, namely[2,3]

$$B_n=H_\pi\sin^2\phi_n+H_\sigma\cos^2\phi_n=H_\pi+(H_\sigma-H_\pi)\cos^2\phi_n\ . \tag{1.3}$$

In this equation the fields H_π and H_σ arise physically from overlap distortions of the "central" cation s orbitals caused by the ligand p orbitals which have been unpaired by spin transfer via π and σ bonds into unoccupied $3d$ orbitals on the neighboring cations n.

In this paper we first demonstrate (Secs. II and III) that, although the *mean* value of H_{hf} in amorphous yttrium iron garnet (a-YIG) is dominated by H_{loc}, the fluctuations ΔH_{hf} which generate the *distribution* of H_{hf} about its average are almost exclusively due to fluctuations in the supertransferred field component $H_{ST}=\vec{H}_{ST}\cdot(\vec{S}_0/S)$. These fluctuations are primarily caused by the local spin disorder of the spin-glass (or speromagnetic) arrangement of frozen spins at low temperatures. Since this same spin disorder determines the local exchange fields H_{ex}, it follows that H_{ST} and H_{ex} are intimately related and that the hyperfine-field distribution indirectly contains a wealth of information concerning the distribution of *exchange* fields as well as the supertransferred hyperfine fields.

A theory is presented (Secs. IV and V) which relates H_{ex} and H_{ST} through the common local spin disorder. Starting from a zeroth-order approximation of a fully frustrated spin model in which $H_{ex}=0$ at every iron site, small self-consistent angular spin perturbations are introduced to simulate the magnetically stable spin-glass order with $\vec{H}_{ex}\|\vec{S}_0$ at each site. In particular, we postulate a functional relationship $H_{ex}\sim f(H_{ST})$ between these fields

and establish that the hyperfine-field distribution can be cast in terms of this function f. Qualitative physical arguments dictate that f should be a single-peaked symmetric function centered at $H_{ST}=0$ and a simple trial Gaussian is found, via the associated theory, to provide an excellent interpretation of the details of the observed hyperfine-field distribution in a-YIG at 4.2 K (Sec. VI).

Using this fit, we are then able to extract from the formalism the actual distribution of exchange fields present in the spin-glass phase of a-YIG (Sec. VI). In particular, we calculate the mean exchange field $\langle H_{ex} \rangle$ and find it to be only about 6% of its equivalent in ferrimagnetic crystalline YIG. This estimate conforms nicely with the observed $\sim$15-fold difference in spin-ordering temperature between crystalline and amorphous YIG. The analytic form of the theory is set out in some generality and should be directly applicable to other amorphous speromagnetic insulators such as FeF_3, $KFeF_4$, etc., which undergo spin-freezing transitions at low temperatures.

II. CRYSTALLINE YIG (c-YIG)

The first really quantitative study of bond-length and bond-angle dependence of hyperfine fields was carried out for Fe^{3+} in octahedral coordination using the rare-earth orthoferrites.[2,4,5] Not only was the validity of the angular dependence of Eq. (1.3) confirmed,[2,4] but a calculation was also presented (using certain proportionality constants obtained from the series of orthoferrite measurements) which related both H_{loc} and isomer shift δ at temperature $T=0$ to the octahedral (iron-oxygen) ligand bond length L. When plotted as H_{loc} versus δ, the essentially linear relationship shown in Fig. 1 is obtained, where the open triangle is the evaluation for $L=2.00$ Å which is the bond length appropriate for the octahedral iron site in c-YIG. The linearity of this plot is anticipated on rather general grounds,[3] but its quantitative relevance in the YIG context can be supported on other wholly independent grounds.

Crystalline YIG has two crystallographically inequivalent Fe^{3+} sites with tetrahedral (d site) and octahedral (a site) oxygen-ligand coordination, respectively.[6] Below the magnetic ordering temperature $T_C=559$ K each ferric $S=\frac{5}{2}$ spin at a d site (a site) is bridged to four (six) antiparallel nearest-neighbor spins via identical Fe—O—Fe ligand bridges with bond angle $\phi \approx 126°$. However, the bond length $L=1.88$ Å at the d sites is shorter than that (≈ 2.00 Å) at the a sites reflecting the greater covalence of the tetrahedral bonding geometry.

Thus, for both sites H_{ST} enhances the local field H_{loc}, both being antiparallel to the electronic spin at the site in question. The dipolar fields H_{dip} are small compared to H_{ST} and H_{loc} but are also collinear with them. At very low temperatures the total hyperfine fields at the two sites are directly measurable as [see Ref. 7 and the results of our own Mössbauer measurements as set out in Table I and Fig. 2(a)]

$$H_{hf}^{(d)}=-473(1)\ \text{kOe},\quad H_{hf}^{(a)}=-552(2)\ \text{kOe}\ , \tag{2.1}$$

where positive fields are (arbitrarily) measured parallel to the electronic spin at the site in question. Relevant dipolar contributions $H_{dip}^{(d)} \approx +2$ kOe and $H_{dip}^{(a)} \approx -8$ kOe can be directly[8] computed from the known spin structure making [from Eq. (1.1)]

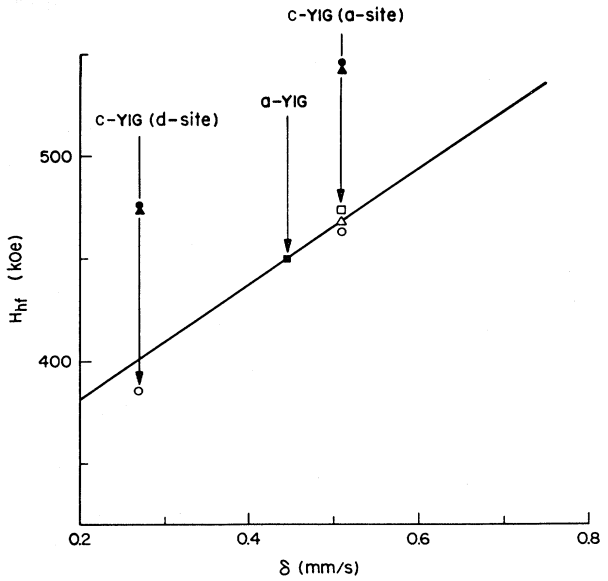

FIG. 1. Estimates and measurements of saturated local contributions H_{loc} (open symbols) and total hyperfine field H_{hf} (solid symbols) as functions of isomer shift δ in YIG. The linear plot is taken from estimates (Ref. 2) made for *octahedral* oxygen coordinations of varying bond lengths L. The open triangle on this line is for $L=2.00$ Å, the bond length for the octahedral a site in c-YIG. The open square and circle at the same value of δ (where the isomer shifts are all arbitrarily measured with respect to iron metal at room temperature) are, respectively, independent experimental (Ref. 9) and theoretical (Ref. 8) estimates for the a site in c-YIG taken from the literature. The open circle at $\delta=0.27$ mm/s is a corresponding theoretical estimate (Ref. 8) for the tetrahedral d site in c-YIG, while the solid circles (triangles) are measured NMR (Mössbauer) values at $T=4.2$ K for total H_{hf} (corrected for small dipolar fields, see text) at these same two c-YIG sites, taken from Table I. Finally, the solid square is the measured low-temperature mean value of isomer shift and total H_{hf} in amorphous YIG (Ref. 10 and Table I).

$$H_{loc}^{(d)}+H_{ST}^{(d)}=-475(1)\ \text{kOe}\ , \tag{2.2}$$

$$H_{loc}^{(a)}+H_{ST}^{(a)}=-544(2)\ \text{kOe}\ , \tag{2.3}$$

which are plotted in Fig. 1 as solid circles (from Ref. 7) or solid triangles (from Table I).

For the a site a direct measure of $H_{ST}^{(a)}$ is available from measurements[9] on garnets in which diamagnetic V^{5+} can substitute for iron in from zero to six of the d sites surrounding an octahedrally coordinated Fe^{3+} in a random fashion. Experiments performed at $T=410$, 300, and 120 K, when extrapolated to $T=0$, give $H_{ST}^{(a)} \approx -70$ kOe for the sum contribution from all six antiparallel nearest-neighbor (NN) spins. The inference, from (2.3), is that $H_{loc}^{(a)} \approx -475$ kOe. This point is also plotted on Fig. 1 (open square) and is in excellent accord with the estimate from the orthoferrite work.[2]

Further confirmation can also be found in the literature from the very recent *ab-initio* molecular-orbital calcula-

TABLE I. Mössbauer hyperfine fields H_{hf}, isomer shifts δ, and linewidths (half width at half maximum, HWHM) for crystalline YIG at 4.2 and 300 K are compared with their equivalents for amorphous YIG at 4.2 K taken from Ref. 10. Also given for comparison are the 4.2 K hyperfine fields for crystalline YIG as measured by NMR (Ref. 7). Crystalline HWHM approximate the value 0.20 mm/s expected for natural linewidth while the amorphous HWHM, which include site-to-site variations of all Mössbauer variables, are much larger. All isomer shifts were measured with respect to iron metal at room temperature.

	iron site	H_{hf}(kOe)	δ(mm/s)	HWHM(mm/s)
4.2 K Mössbauer	*a* site	550	0.51	0.18
c-YIG	*d* site	472	0.27	0.21
300 K Mössbauer	*a* site	488	0.38	0.23
c-YIG	*d* site	395	0.16	0.23
4.2 K Mössbauer	site-	450	0.45	0.5–0.7
a-YIG	averaged			
4.2 K NMR	*a* site	554		
c-YIG	*d* site	473		

tions[8] performed on *c*-YIG itself, using clusters of up to 62 ions. They provide estimates for the ratio H_{ST}/H_{loc} of 0.233 (*d* sites) and 0.174 (*a* sites) which, when scaled to the total measured values of Eqs. (2.2) and (2.3), give

$$H_{loc}^{(d)} \approx -385 \text{ kOe}, \quad H_{ST}^{(d)} \approx -90 \text{ kOe}, \tag{2.4}$$

$$H_{loc}^{(a)} \approx -463 \text{ kOe} \quad H_{ST}^{(a)} \approx -81 \text{ kOe}, \tag{2.5}$$

the local components being shown as open circles in Fig. 1. The fact that the supertransferred component *per antiparallel NN spin* is significantly larger ($\approx$23 kOe) for the tetrahedral *d* site than that ($\approx$13 kOe) for the octrahedral *a* site is anticipated, and results from the larger covalency of the *d* sites. What is surprising is the fact that the $H_{loc}^{(d)}$ value also falls close to the linear H_{loc} versus δ relationship which was derived for octahedral coordination (see Fig. 1). It suggests that this line may be approximately relevant for more general iron-oxygen local coordinations of high symmetry.

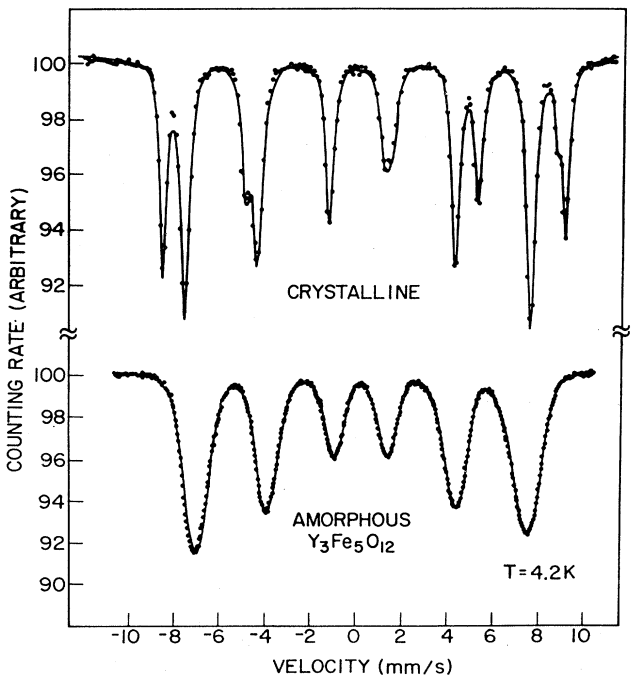

FIG. 2. ^{57}Fe Mössbauer absorption spectra for (a) crystalline and (b) amorphous YIG obtained at $T=4.2$ K in standard transmission geometry with a conventional constant acceleration spectrometer using a ^{57}Co in Pd source. The solid lines are the best fits to the data using a three-site Lorentzian-line interpretation for (a) and a symmetric Gaussian distribution of natural Lorentzians for (b). The small difference between the two (rigorously inequivalent) octahedral sites in (a) has been ignored in the text of this paper and in Table I.

III. AMORPHOUS YIG(*a*-YIG)

In its amorphous form, $Y_3Fe_5O_{20}$ exhibits only a single broad distribution of isomer shifts and hyperfine fields below the spin-freezing temperature [Fig. 2(b)]. Thus, although we shall refer to it as *a*-YIG, no memory of the garnet crystalline structure (with its two very different inequivalent iron sites) is retained. At liquid-helium temperature the broad amorphous-phase distributions are centered closely on the mean values[10]

$$\langle H_{hf} \rangle = -450 \text{ kOe}, \quad \langle \delta \rangle = 0.446 \text{ mm/s}, \tag{3.1}$$

the isomer shift here (and elsewhere in this paper) being measured with respect to that of iron metal at room temperature.

By virtue of the amorphous matrix and "spin-glass" disorder of magnetic moments, mean dipolar contributions $\langle H_{dip} \rangle$ to total mean hyperfine field are almost certainly smaller than their already small crystalline equivalents. They are correspondingly neglected. It then follows from Eq. (3.1) that

$$\langle H_{loc} \rangle + \langle H_{ST} \rangle = -450 \text{ kOe}, \tag{3.2}$$

and this value is shown in Fig. 1 by the solid square. It is immediately apparent from Fig. 1 that the mean supertransferred field $\langle H_{ST} \rangle$ in *a*-YIG must be very close to zero. Thus, while the (solid circle or triangle) values of $H_{loc}+H_{ST}$ for each crystalline site are $\sim$80–90 kOe above the H_{loc} versus δ line, the equivalent point (solid square) for *a*-YIG is right on this line.

Physically this can only mean that the spin-glass disorder of speromagnetic *a*-YIG is such that spins are almost fully orientationally disordered *even on a local (NN) scale,*

this in spite of the very dominant antiferromagnetic exchange present (as evidenced by the large negative magnetic Curie-Weiss temperature seen in the higher-temperature paramagnetic phase[11]). We conclude that

$$\langle H_{\rm ST}\rangle \approx 0\ ,\langle H_{\rm loc}\rangle = -450\ \text{kOe},\ \ a\text{-YIG}\ , \tag{3.3}$$

where scalar values of hyperfine field are measured along the direction of local spin $\vec{S}_0$, i.e., $H_{\rm ST}=\vec{H}_{\rm ST}\cdot(\vec{S}_0/S)$.

Also determined from our earlier Mössbauer-Zeeman analysis[10] of a-YIG at 4.2 K were the standard deviation $\sigma(x)\equiv\langle(\Delta x)^2\rangle^{1/2}$; $\Delta x\equiv x-\langle x\rangle$ for $x=\delta$ and $x=H_{\rm hf}$ as follows:

$$\sigma(\delta)=0.21\ \text{mm/s},\ \ \sigma(H_{\rm hf})=29\ \text{kOe}\ , \tag{3.4}$$

and the correlation

$$\langle\Delta\delta\Delta H_{\rm hf}\rangle = 0.18\sigma(\delta)\sigma(H_{\rm hf})\ . \tag{3.5}$$

Now the fluctuations $\Delta\vec{H}_{\rm hf}\approx\Delta\vec{H}_{\rm loc}+\Delta\vec{H}_{\rm ST}$ are composed of two components of quite different character. At or near spin saturation $|\vec{S}_0|=S$, $\Delta H_{\rm loc}$ results dominantly from variations of d-electron population via overlap and spin transfer with ligand p orbitals at the iron site in question.[2,3] These same overlap and transfer terms also dominate the isomer shift fluctuations $\Delta\delta$, leading to anticipated strong correlations between $\Delta H_{\rm loc}$ and $\Delta\delta$. In contrast, fluctuation $\Delta\vec{H}_{\rm ST}$ is the vector sum of components from all NN spins $\vec{S}_n$, each component being parallel to that spin. These NN "frozen" spins $\vec{S}_n$ are pseudorandomly oriented on a local scale in a-YIG, and this orientational randomness will therefore give rise to large fluctuations $\Delta H_{\rm ST}$ which are largely independent of isomer shift or local hyperfine field. We therefore anticipate the relationships

$$\sigma(H_{\rm hf})=[\sigma^2(H_{\rm loc})+\sigma^2(H_{\rm ST})]^{1/2}\approx 29\ \text{kOe}\ , \tag{3.6}$$

$$\langle\Delta H_{\rm ST}\Delta\delta\rangle\approx 0\ , \tag{3.7}$$

$$\langle\Delta H_{\rm loc}\Delta\delta\rangle = b\sigma(H_{\rm loc})\sigma(\delta)\ , \tag{3.8}$$

where $b\lesssim 1$, $b=1$ corresponding to full linear correlations between the variables involved.[12] Equation (3.6) assumes the statistical independence of $\Delta H_{\rm loc}$ and $\Delta H_{\rm ST}$, and Eq. (3.7) assumes the statistical independence of $\Delta H_{\rm ST}$ and $\Delta\delta$.

If we set $b=1$ in Eq. (3.8) and utilize (3.5) and (3.7), we find

$$\langle\Delta H_{\rm hf}\Delta\delta\rangle=\langle\Delta H_{\rm loc}\Delta\delta\rangle=\sigma(H_{\rm loc})\sigma(\delta)=0.18\sigma(H_{\rm hf})\sigma(\delta)\ , \tag{3.9}$$

leading to $\sigma(H_{\rm loc})/\sigma(H_{\rm hf})=0.18$ or, via Eq. (3.6),

$$\sigma(H_{\rm ST})/\sigma(H_{\rm hf})=[1-(0.18)^2]^{1/2}\approx 0.98\ . \tag{3.10}$$

Even if b is as small as 0.3 (representing only minor correlations between $\Delta H_{\rm loc}$ and $\Delta\delta$) the overwhelming dominance of supertransferred hyperfine field is maintained with $\sigma(H_{\rm ST})$ then making up about 80% of $\sigma(H_{\rm hf})$.

Such a dominance can be independently established from an evaluation of $\sigma(H_{\rm ST})$ directly for a-YIG via the spherical random-packing model[13] which has been successful in other predictions concerning local structure in this material.[14] Thus, from Eqs. (1.2), (1.3), and (3.3) we have

$$\langle(\Delta H_{\rm ST})^2\rangle\approx\langle H_{\rm ST}^2\rangle = \left\langle\left[\sum_n [H_\pi+(H_\sigma-H_\pi)\cos^2\phi_n]\cos\xi_n\right]^2\right\rangle, \tag{3.11}$$

in which the sum $\sum_n$ is over all single-bridged (with bridge-angle ϕ_n) nearest neighbors $\vec{S}_n$ of a representative iron spin $\vec{S}_0$, and $\cos\xi_n=(\vec{S}_0\cdot\vec{S}_n)/S^2$ measures the normalized angular projection of $\vec{S}_n$ upon $\vec{S}_0$.

From the experimental measurements of Freund *et al.*[15] it is known that $H_\sigma\approx 6H_\pi$ for Fe^{3+}—O^{2-} coordination. Also, from (2.4) and (2.5) we know that $H_{\rm ST}$ per antiparallel NN spin in c-YIG (with $\phi_n\approx 126°$)[6] is about 23 kOe for d sites and 13 kOe for a sites. Interpolating linearly between these points on Fig. 1 as a function of δ, we anticipate that a value of about 16 kOe should be approximately valid for the evaluation of $H_{\rm ST}$ per antiparallel NN spin with $\phi\approx 126°$ at a value of δ corresponding to a-YIG. In other words, the relationship

$$H_\pi+(H_\sigma-H_\pi)\cos^2(126°)=16\ \text{kOe}\ , \tag{3.12}$$

together with $H_\sigma=6H_\pi$ should provide values of H_σ and H_π appropriate for use in the context of a-YIG. Solving these equations, we obtain

$$H_\sigma\approx 35\ \text{kOe},\ \ H_\pi\approx 6\ \text{kOe}\ . \tag{3.13}$$

Now within the model of Ref. 13, the probability distribution for ϕ_n approximates $\sin\phi_n$ with $\pi/2\lesssim\phi_n<\pi$, while the mean (and most probable) number of NN spins n is five [see Figs. 12 and 14(a) of Ref. 13]. Therefore, using (3.11) in a random spin orientation approximation, we can directly derive

$$\langle(\Delta H_{\rm ST})^2\rangle=(H_\sigma-H_\pi)^2\left\langle\sum_n[(\cos^2\phi_n+t)\cos\xi_n]^2\right\rangle\ , \tag{3.14}$$

where $t=H_\pi/(H_\sigma-H_\pi)=0.2$, as

$$\sigma^2(H_{\rm ST})=\frac{5(H_\sigma-H_\pi)^2\int_0^\pi\int_{\pi/2}^\pi(\cos^4\phi+2t\cos^2\phi+t^2)\cos^2\xi\sin\phi\sin\xi\,d\phi\,d\xi}{\int_0^\pi\int_{\pi/2}^\pi\sin\phi\sin\xi\,d\phi\,d\xi}$$

$$=\tfrac{5}{3}(H_\sigma-H_\pi)^2(t^2+2t/3+\tfrac{1}{5})=0.6222(H_\sigma-H_\pi)^2\ . \tag{3.15}$$

With the use of (3.13) this produces the estimate $\sigma(H_{ST})\approx 23$ kOe for a-YIG to be compared with the total hyperfine width $\sigma(H_{hf})$ of 29 kOe.

Thus, the conclusions from Secs. II and III for a-YIG are that the *average* value of H_{hf} in a-YIG is essentially that of H_{loc} while the distribution ΔH_{hf} about this average is dominated by ΔH_{ST}.

IV. INFLUENCE OF THE EXCHANGE FIELD

An arbitrary ferric ion in a-YIG is subject to two separate magnetic fields. In addition to $\vec{H}_{hf}$ which acts on the nuclear spin, an exchange field $\vec{H}_{ex}$ acts on the electronic spin $\vec{S}_0$. The latter, which by definition determines the direction of $\vec{S}_0$, is parallel to $\vec{S}_0$ and is composed of an antiferromagnetic kinetic[16] contribution[3]

$$\vec{H}_{ex}\propto \sum_n [2H_\pi+(H_\sigma-2H_\pi)\cos^2\phi_n](\vec{S}_n/S)\ , \tag{4.1}$$

and a ferromagnetic (potential)[16] one. The former, Eq. (4.1), dominates in a-YIG at all bond angles ϕ_n except possibly those close to $\phi_n=\pi/2$ for which the situation is uncertain.

In spite of the similarity in form of their individual components (1.3) and (4.1), the resultant $\vec{H}_{hf}$ and $\vec{H}_{ex}$ are by no means trivially related in the amorphous context. In particular, since $\langle H_{ST}\rangle\approx 0$ in a-YIG [Eq. (3.3)], $\vec{H}_{ex}$ and $\vec{H}_{ST}$ must be approximately randomly oriented relative to each other in the glass. The situation is depicted schematically in Fig. 3. More precisely, however, this randomness cannot be exact since it would result in an exactly symmetric distribution of hyperfine fields. Nor can the spins themselves be *exactly* randomly oriented since such a configuration would not produce an exchange field parallel to $\vec{S}_0$ except in rare fortuitous instances.

A useful starting approximation in describing the actual spin-glass order is that of a completely frustrated[17] network defined by the condition

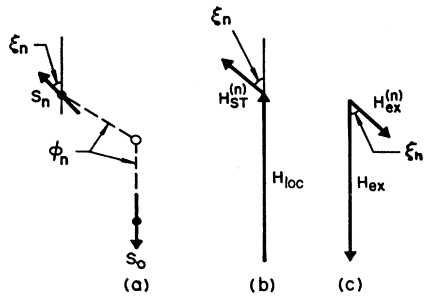

FIG. 3. (a) Schematic for a ferric iron-oxygen-iron ligand bridge (of bond angle ϕ_n) between a central cation with electronic spin $\vec{S}_0$ and one of its cation nearest neighbors $\vec{S}_n$ in the spin-glass (or speromagnetic) phase of a-YIG. (b) The directions of the resulting local H_{loc} and supertransferred $H_{ST}^{(n)}$ components of hyperfine field experienced by the nucleus of the central cation. (c) The corresponding directions of the exchange field $H_{ex}^{(n)}$ and total vector resultant exchange $H_{ex}=\sum_n H_{ex}^{(n)}$. The latter, for self-consistency, must be parallel to central spin $\vec{S}_0$.

$$g\mu_B\vec{H}_{ex}^{0}=\sum_n 2J_n\vec{S}_n^{0}=0\ , \tag{4.2}$$

in which J_n is an exchange parameter defined by the NN exchange Hamiltonian

$$\mathscr{H}=-\sum_n 2J_n\vec{S}_0\cdot\vec{S}_n=-g\mu_B\vec{H}_{ex}\cdot\vec{S}_0 \tag{4.3}$$

and the zeroth-order approximation in (4.2) is symbolized by the zero superscript. This configuration evidently has no exchange stability and must therefore be perturbed in a manner which produces stability in a self-consistent manner. Let us consider the situation in more detail.

Using Eqs. (1.2), (1.3), and (4.1), with $H_\pi\ll H_\sigma$, we adopt the notation

$$\vec{H}_{ex}=\sum_n 2J_n\vec{S}_n\ , \tag{4.4}$$

$$\vec{H}_{ST}=A\sum_n 2(J_n+\epsilon_n)\vec{S}_n=A\left[\vec{H}_{ex}+\sum_n 2\epsilon_n\vec{S}_n\right]\ , \tag{4.5}$$

in which $\epsilon_n\ll J_n$, A is a numerical constant, and J_n is expressed in field units. In zeroth order, using (4.2), we find

$$\vec{H}_{ST}^{0}=A\sum_n 2(J_n+\epsilon_n)\vec{S}_n^{0}=A\sum_n 2\epsilon_n\vec{S}_n^{0}\ . \tag{4.6}$$

Also, assuming hyperfine-field fluctuations to be dominated by supertransferred contributions, as established in Sec. III,

$$\Delta H_{hf}^{0}=\vec{H}_{ST}^{0}\cdot(\vec{S}_0/S)=|H_{ST}^{0}|\cos\xi\ , \tag{4.7}$$

in which ξ is the angle between $\vec{H}_{ST}^{0}$ and $\vec{S}_0$.

As a first-order correction to the fully frustrated spin network we perturb the NN spins of each central site $\vec{S}_0$ in the fashion

$$\vec{S}_n=\vec{S}_n^{0}-d_n\vec{S}_0\ , \tag{4.8}$$

such that each acquires an additional small component ($d_n\ll 1$) antiparallel to $\vec{S}_0$. These small perturbations result in small stabilizing exchange fields parallel to $\vec{S}_0$ and simulate local spin-glass ordering in a highly frustrated system dominated by antiferromagnetic (J_n negative) exchange. After the perturbation we find, by direct substitution into (4.4) and (4.5),

$$\vec{H}_{ex}=-\sum_n 2J_nd_n\vec{S}_0\ , \tag{4.9}$$

$$\vec{H}_{ST}=A\sum_n(2\epsilon_n\vec{S}_n^{0}-2J_nd_n\vec{S}_0)=\vec{H}_{ST}^{0}+A\vec{H}_{ex}\ , \tag{4.10}$$

where we work to first order of smallness in d_n and ϵ_n/J_n. The resulting contribution to hyperfine distribution is

$$H_{ST}=\vec{H}_{ST}\cdot(\vec{S}_0/S)=AH_{ex}+|H_{ST}^{0}|\cos\xi\ . \tag{4.11}$$

Taking the angle ξ between $\vec{H}_{ST}^{0}$ and $\vec{S}_0$ to be closely a random variable leads directly to a most important finding, namely

$$\langle H_{ST}\rangle=A\langle H_{ex}\rangle\ . \tag{4.12}$$

In other words, the mean value of the supertransferred component of hyperfine field, when averaged over all iron sites, provides a direct measure of the mean exchange field averaged over the same sites.

V. HYPERFINE LINE SHAPE (THEORY)

In the fully frustrated zeroth-order limit of Sec. IV with $H_{ex}=0$ we have, from Eq. (4.11),

$$H_{ST}^0 = |H_{ST}^0| \cos\xi \ , \tag{5.1}$$

with ξ a closely random variable. The resulting probability distribution $p_0(H_{ST}^0)$ is symmetric and will be assumed Gaussian, viz,

$$p_0(H_{ST}^0)=\exp[-(H_{ST}^0/w_0)^2] \ , \tag{5.2}$$

in which w_0 is a width parameter. From Eq. (4.11) we see that exchange perturbations of the zeroth-order configuration increase the magnitude of H_{ST}^0 at every iron site. However, the magnitude of this increment AH_{ex} is by no means independent of the angle ξ. For example, if all NN spins at a particular site are quasiparallel or antiparallel to $\vec{S}_0$ in zeroth order ($\cos\xi\approx\pm1$) small angular perturbations cannot enhance H_{ex} in first order. At the opposite extreme of all NN spins quasiperpendicular to $\vec{S}_0$ ($\cos\xi\approx0$) small angular perturbations produce their maximum first-order exchange-field enhancements. More generally, a significant inverse correlation is anticipated between H_{ex} and the magnitude of the projection of $\vec{H}_{ST}$ on $\vec{S}_0$. Let us suppose that it can be at least approximately cast in a simple functional form. Accordingly we write the increment AH_{ex} in the form

$$AH_{ex}=cf(H_{ST}) \ , \tag{5.3}$$

where c is a constant and f is a symmetric function single peaked at $H_{ST}=0$, and (arbitrarily) normalized to unity at its peak.

From (4.11), (5.1), and (5.3) we now have

$$H_{ST}=H_{ST}^0+cf(H_{ST}) \ . \tag{5.4}$$

The resulting hyperfine line shape, to the extent that it is dominated by supertransferred fluctuations, follows from Eqs. (5.2) and (5.4) as

$$p(H_{ST})=\exp\{-[H_{ST}-cf(H_{ST})]^2/w_0^2\} \ . \tag{5.5}$$

Assuming $c \ll w_0$, and working to first order in c/w_0, we can now derive by direct integration the mean values of H_{ST} and H_{ST}^2 over this distribution. They are

$$\langle H_{ST}\rangle=(2c/w_0^2)\langle h^2 f(h)\rangle_0 \ , \tag{5.6}$$

$$\langle H_{ST}^2\rangle=w_0^2/2 \ , \tag{5.7}$$

in which $\langle h^2 f(h)\rangle_0$ refers to an average over the distribution $p_0(h)=\exp(-h^2/w_0^2)$ of Eq. (5.2).

Experimentally $p(h)$, $h=\Delta H_{hf}\approx H_{ST}$, is deduced from the shapes of the outside lines L_1 and L_6 of the ^{57}Fe Mössbauer spectrum, and its form has been detailed[18,19] by using a minimum least-squares fit to a symmetric Gaussian $p_G(h)$ and recording the residual $r(h)$. This residual is therefore of the form

$$r(h)=p(h)-\exp[-(h-d)^2/w_0^2] \ . \tag{5.8}$$

Using Eq. (5.5) with $h=H_{ST}$, this can be recast in the form

$$r(h)=(2h/w_0^2)[cf(h)-d]e^{-h^2/w_0^2} \ , \tag{5.9}$$

to first order in c/w_0 and d/w_0, and is an odd function of h which passes through zero at $h=0$.

A fit of $r(h)$ to the measured residual should therefore furnish us with the single-peaked (about $h=0$) symmetric function $f(h)$ together with the constants w_0, c, and d. An obvious, and as it turns out quite realistic, guess for $f(h)$ is a symmetric Gaussian form

$$f(h)=e^{-\alpha^2h^2/w_0^2} \ , \tag{5.10}$$

in terms of which the residual $r(h)$ of (5.9) becomes

$$r(h)=(2hc/w_0^2)e^{-h^2/w_0^2}[e^{-\alpha^2h^2/w_0^2}-(d/c)] \ . \tag{5.11}$$

This is now an odd function of h which passes through zero three times, at $-h_0$, 0, and $+h_0$, where

$$d/c=e^{-\alpha^2h_0^2/w_0^2} \ . \tag{5.12}$$

The substitution of (5.12) into (5.11) provides us with our final form for the residual, viz,

$$r(h)=(2hc/w_0)e^{-h^2}(e^{-\alpha^2h^2}-e^{-\alpha^2h_0^2}) \ , \tag{5.13}$$

in which h and h_0 are now and henceforth to be measured in units of w_0. It follows that the reduced residual $(w_0/c)r(h)$ is a function of the two parameters h_0 and α. However, in the present context even these are necessarily related since the least-mean-squares minimization pro-

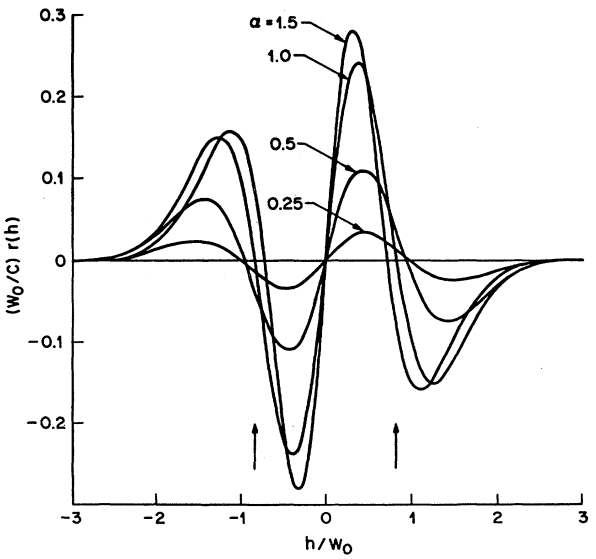

FIG. 4. Reduced residual $(w_0/c)r(h)$, representing the predicted deviation of hyperfine line shape from the best least-squares symmetric Gaussian fit, from Eq. (5.17) of the text. A family of residuals is shown for different values of the single adjustable parameter α involved, and the arrows mark the half width at half height of the associated "best-fit" parent symmetric Gaussian.

cedure essentially adjusts $r(h)$ to have closely equal integrated positive and negative areas, i.e.,

$$\int_{-\infty}^{\infty} r(h)dh = 0 , \tag{5.14}$$

from which, directly integrating (5.13), we derive the condition

$$\alpha^2 h_0^2 = \ln(1+\alpha^2) , \tag{5.15}$$

or, equivalently,

$$h_0 = \pm(w_0/\alpha)[\ln(1+\alpha^2)]^{1/2} . \tag{5.16}$$

Our final form for the *reduced* residual, based solely on the presumed Gaussian distribution f of exchange fields via the Eq. (5.3), is therefore

$$(w_0/c)r(h) = 2he^{-h^2}[e^{-\alpha^2 h^2} - 1/(1+\alpha^2)] . \tag{5.17}$$

It involves only the single parameter α and is plotted for several values of α in Fig. 4.

VI. HYPERFINE LINE SHAPE (FIT FOR a-YIG)

The experimental line shape $p(h)$ for a-YIG [Ref. 10 and Fig. 2(b)] resolved into its best-fit symmetric Gaussian $p_G(h)$ and residual $r(h)$ components,[18] is shown in Fig. 5. The experimental residual obviously bears a strong resemblance to the family of theoretical residuals of Fig. 4. It is closely antisymmetric about its center $h=0$ and has h_0 equal to about 1.1 times the half width at half height of $p_G(h)$, i.e., $h_0 \approx 1.1(\ln 2)^{1/2} w_0 \approx 0.9 w_0$. From (5.16) we conclude that $\alpha \approx 0.7$ is appropriate for a-YIG. The corresponding fit of the theoretical residual (5.17) to the experimental $r(h)$ is shown in Fig. 5(b). From its amplitude we find

$$c/w_0 \approx 0.20 , \tag{6.1}$$

and, in combination with Eq. (5.12), $d/w_0 \approx 0.13$. These small values justify our working to only first order in these parameters when calculating the functional form of the residual.

The quantitative deviations between theory and experiment seen in Fig. 5(b) are thought to involve the existence of "tail" states[19] in the hyperfine distribution at 4.2 K which should disappear as $T \to 0$. These effects will be discussed in some detail, both in the context of a-YIG and other amorphous speromagnetic insulators, in a future publication. Neglecting this additional complexity, which does not seriously affect the conclusion (6.1), we can now, via Eqs. (5.3) and (5.10), proceed to calculate the mean exchange energy in the form

$$\begin{aligned} A\langle H_{ex}\rangle = c\langle f(h)\rangle &= \int_{-\infty}^{\infty} ce^{-\alpha^2 h^2} e^{-h^2} dh \Big/ \int_{-\infty}^{\infty} e^{-h^2} dh \\ &= c/(1+\alpha^2)^{1/2} \\ &= 0.2 w_0/(1+\alpha^2)^{1/2} . \end{aligned} \tag{6.2}$$

Since from (5.7) $w_0 = \sqrt{2}\sigma(H_{ST})$, and $\sigma(H_{ST}) \approx 23$ kOe from Sec. III, we conclude from (6.2) with $\alpha = 0.7$ that

$$w_0 \approx 33 \text{ kOe and } A\langle H_{ex}\rangle \approx 5.3 \text{ kOe} , \tag{6.3}$$

in a-YIG.

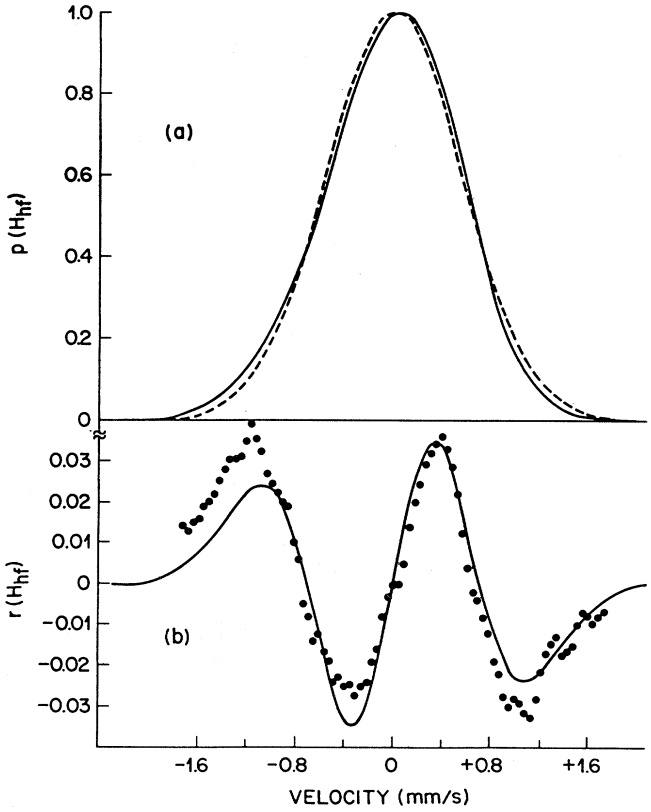

FIG. 5. Measured hyperfine-field distribution $P(H_{hf})$, solid line, and its best-fit symmetric Gaussian approximation $p_G(H_{hf})$, dashed line, as deduced from the combined outside line shapes of the 4.2 K ^{57}Fe Mössbauer-Zeeman spectrum of a-YIG (Ref. 18). (b) The actual Mössbauer data per channel (solid circles) for the experimental residual $r(H_{hf}) = p(H_{hf}) - p_G(H_{hf})$ and the theoretical curve (solid line) from Eq. (5.17) of the text for $\alpha = 0.7$. The abscissa is given in Mössbauer velocity units.

The parameter A, which relates supertransferred and exchange fields via Eqs. (4.4) and (4.5), can be adequately estimated in the present context from the ratio $|H_{ST}/H_{ex}|$ in c-YIG. We have already estimated $|H_{ST}| \approx (85 \pm 5)$ kOe in Sec. II [Eqs. (2.4) and (2.5)] and H_{ex} follows from Wojtowicz's[20] value of $J \approx -33$ K for c-YIG as

$$H_{ex} = -2JzS/g\mu_B \approx 6.1 \text{ MOe}, \quad c\text{-YIG} \tag{6.4}$$

where $g=2$, $S=\frac{5}{2}$ and the average number of NN $z \approx 5$. It follows that $A \approx 0.014$ and that, consequently, from (6.3)

$$\langle H_{ex}\rangle \approx 380 \text{ kOe}, \quad a\text{-YIG} . \tag{6.5}$$

Comparing (6.4) and (6.5) we see that the mean exchange field stabilizing the speromagnetic order in a-YIG is only about 6.2% of that which stabilizes the ferrimagnetic order in c-YIG. With this evidence one might therefore perhaps anticipate a spin-glass ordering temperature T_{SG} in a-YIG of order 0.062 times the Curie temperature $T_C = 559$ K of c-YIG, which is about 35 K. Experimentally,[11] T_{SG} is not precisely known but is thought to be in the region of 40 K.

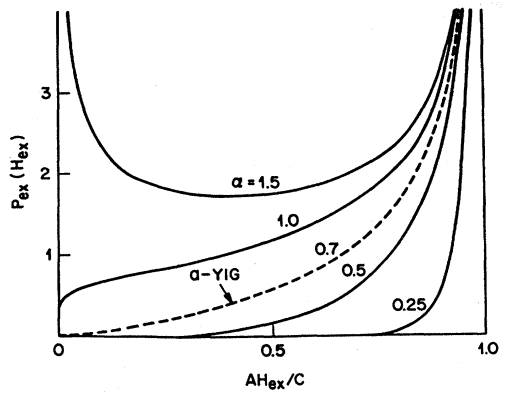

FIG. 6. The unnormalized distribution $p_{ex}(H_{ex})$ of exchange fields in an amorphous ferric speromagnetic insulator as $T\rightarrow 0$ from the theory of the present paper, i.e., Eq. (6.8) of the text. A family of distributions is shown as a function of the single adjustable parameter α involved and includes that ($\alpha=0.7$) relevant for a-YIG.

We can now proceed further to calculate the predicted analytic form of the distribution function $p_{ex}(H_{ex})$ of exchange field in a-YIG. From Eqs. (5.3) and (5.10) we have

$$H_{ex}=(c/A)e^{-\alpha^2 h^2/w_0^2},\quad h=H_{ST} \tag{6.6}$$

while, in zeroth order, the distribution of supertransferred field components is

$$p_0(h)=e^{-h^2/w_0^2},\quad h=H_{ST}\ . \tag{6.7}$$

From these equations the exchange distribution function follows directly as

$$p_{ex}(H_{ex})=p_0(h)\frac{dh}{dH_{ex}}=NH_{ex}^{(1-\alpha^2)/\alpha^2}[\ln(c/AH_{ex})]^{-1/2} \tag{6.8}$$

in which N is merely a normalizing constant. If $\alpha\leq 1$ this distribution goes to zero as $H_{ex}\rightarrow 0$ and diverges in the limit $H_{ex}\rightarrow c/A$ (which is 470 kOe for a-YIG). The detailed function $p_{ex}(H_{ex})$ from Eq. (6.8) is plotted for several values of α, including that ($\alpha=0.7$) relevant for a-YIG, in Fig. 6.

VII. SUMMARY

We have established that for amorphous YIG at 4.2 K, the *mean* value of hyperfine field is closely that of the local contact component alone while *fluctuations* about this mean are dominantly produced by supertransferred components via the speromagnetic disorder of the frozen spins. We postulate that this situation is common to all ferric speromagnets. We then formulate a theory which relates exchange fields and supertransferred hyperfine fields via the common spin disorder which generates them. Within this formalism both the shape of the distribution of hyperfine fields and the distribution of exchange fields are expressed in terms of a single variable (Figs. 4 and 6). The theory is successfully compared with experiment for the shape of the hyperfine-field distribution in amorphous YIG. The corresponding exchange field distribution exhibits the "exchange hole" for small fields familiar from the computer simulations[21] of more conventional spin glasses.

[1]J. Chappert, Hyperfine Interact. **13**, 25 (1983).
[2]G. A. Sawatzky and F. Van der Woude, J. Phys. (Paris) Colloq. **35**, C6-47 (1974).
[3]B. C. Tofield, J. Phys. (Paris) Colloq. **37**, C6-539 (1976).
[4]C. Boukema, F. Van der Woude, and G. A. Sawatzky, Int. J. Magn. **3**, 341 (1972).
[5]M. Eibschütz, S. Shtrikman, and D. Treves, Phys. Rev. **156**, 562 (1967).
[6]S. Geller and M. A. Gilleo, J. Phys. Chem. Solids **3**, 30 (1957).
[7]J. D. Lister and G. B. Benedek, J. Appl. Phys. **37**, 1320 (1966).
[8]H. Winkler, R. Eisberg, E. Alp, R. Ruffer, E. Gerdau, S. Lauer, A. Trautwein, M. Grodzicki, and A. Vera, Z. Phys. B **49**, 331 (1983).
[9]V. A. Bokov, S. I. Jushchuk, and G. V. Popov, Solid State Commun. **7**, 373 (1969).
[10]M. Eibschütz and M. E. Lines, Phys. Rev. B **26**, 2288 (1982).
[11]E. M. Gyorgy, K. Nassau, M. Eibschütz, J. V. Waszczak, C. A. Wang, and J. C. Shelton, J. Appl. Phys. **50**, 2883 (1979).
[12]M. E. Lines and M. Eibschütz, Solid State Commun. **45**, 435 (1983).
[13]M. E. Lines, Phys. Rev. B **20**, 3729 (1979).
[14]M. E. Lines and M. Eibschütz, Phys. Rev. B **25**, 6042 (1982).
[15]P. Freund, J. Owen, and B. F. Hann, J. Phys. C **6**, L139 (1973).
[16]P. W. Anderson, Solid State Phys. **14**, 99 (1963).
[17]G. Toulouse, Commun. Phys. **2**, 115 (1977).
[18]M. E. Lines, in *Essays in Theoretical Physics,* edited by W. E. Parry (Pergamon, Oxford, 1984).
[19]E. Eibschütz, M. E. Lines, L. G. van Uitert, H. J. Guggenheim, and G. J. Zydzik, Phys. Rev. B **29**, 3843 (1984).
[20]P. J. Wojtowicz, Phys. Lett. **11**, 18 (1964).
[21]L. R. Walker and R. E. Walstedt, Phys. Rev. B **22**, 3816 (1980).